



# Accurate hyperspectral imaging of mineralised outcrops: An example from lithium-bearing pegmatites at Uis, Namibia

René Booysen, Sandra Lorenz, Samuel T. Thiele, Warrick C. Fuchsloch, Timothy Marais,  
Paul A.M. Nex, Richard Gloaguen

Accepted at: *Remote Sensing of Environment*, Elsevier Inc. 2021

## Qualifiers Phase II Presentation

(January 19<sup>th</sup>, 2024)

### DSC Members

Prof. Subramanian Sankaranarayanan  
Prof. Mayank Singh  
Prof. Pankaj Khanna  
Prof. Shanmuganathan Raman

### Presented by

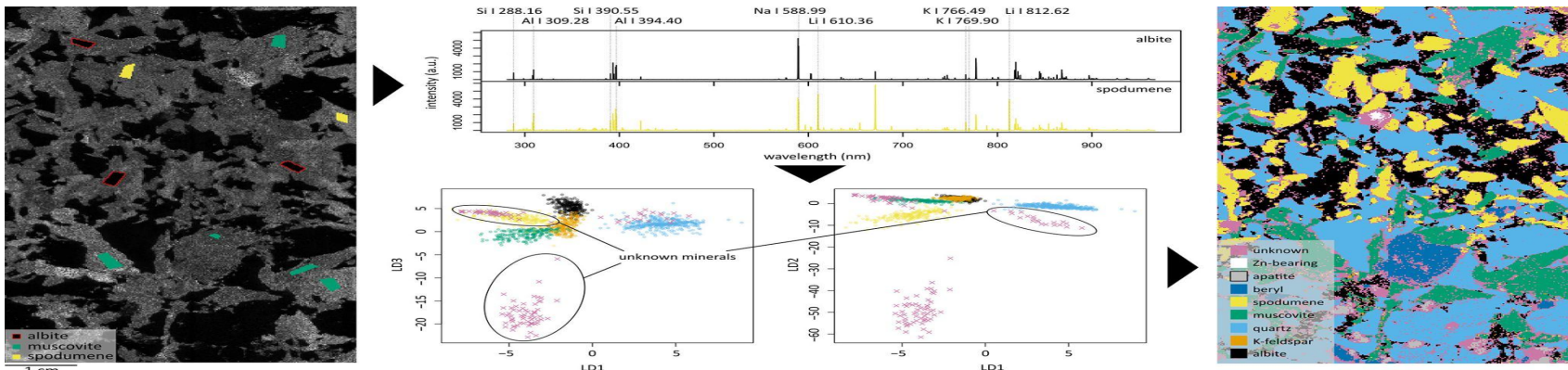
Akbar Ali  
Roll Number: 22310050  
Discipline of Computer Science and engineering

# Contents

- Objective
- Introduction
  - Background
  - Study Focus
- Geological Remote Sensing
  - Introduction to HSI
  - Background of HSI
  - Spectral Signature
  - Wavelength Ranges
- HSI Workflow
  - List of Sensors
  - Limitations
- Ground-Based HSI
- Methodology
  - Study Sites
  - Flow Diagram
- Results
- Challenges
- Future Directions

# 1. Objectives of the Study

The paper proposes an innovative approach that integrates multiple sensors and scales of data acquisition to identify and map lithium-bearing minerals in the Uis pegmatite complex, Namibia, which can be used for efficient mapping of complex terrains and optimization of ore extraction



## 2. Introduction



- In the context of the global green energy transition, the demand for raw materials is experiencing a significant surge.

## 2. Introduction(2)

- Lithium plays a pivotal role in the energy transition as a critical component for manufacturing batteries that power electric vehicles and store renewable energy.
- The green energy transition has surged the demand for raw materials, emphasizing the necessity for sustainable and efficient resource exploration.

## 2.1 Background

- This paper addresses the need for efficient and rapid methods of exploration to discover new deposits and support the green energy transition.
- While recycling rates are improving, the need for new discoveries remains critical to sustain the supply chain (Gandhi and Sarkar, 2016; Ali et al., 2017).

## 2.2 Study Focus

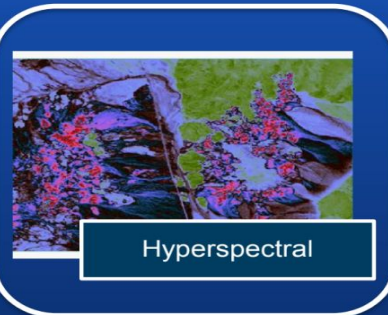
- Study hones in on the Uis region in Namibia, specifically exploring lithium-bearing pegmatites.
- Lithium, a key mineral in the energy transition, has garnered attention, marked as 'critical' by the EU Commission in 2020.

### 3. Geological Remote Sensing

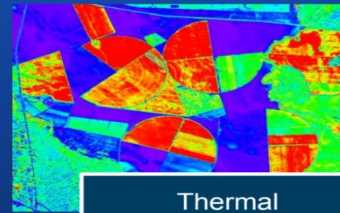
#### Remote Sensing Datasets



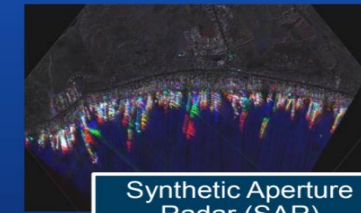
Multispectral



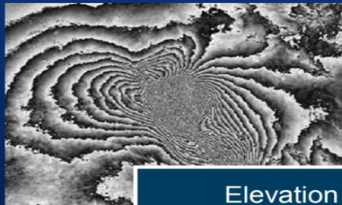
Hyperspectral



Thermal



Synthetic Aperture Radar (SAR)



Elevation



Aerial



Drone

# 3. Geological Remote Sensing(2)

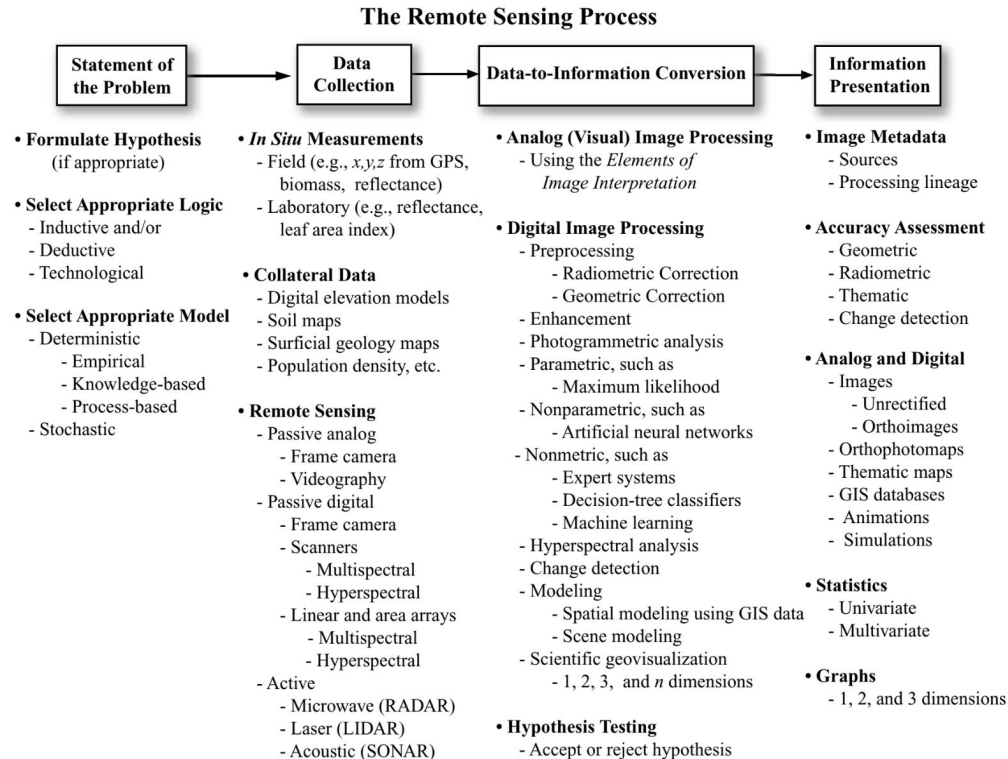
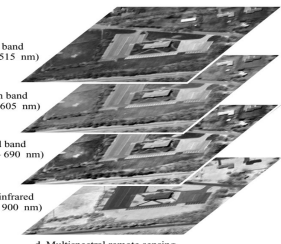
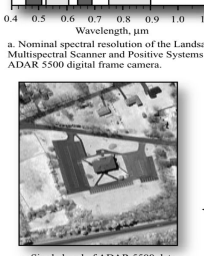
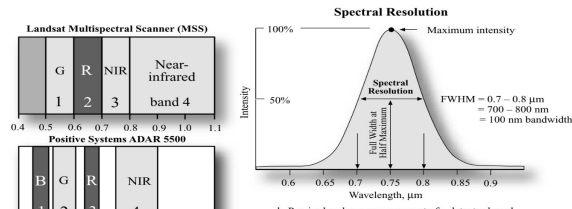
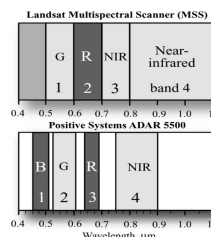
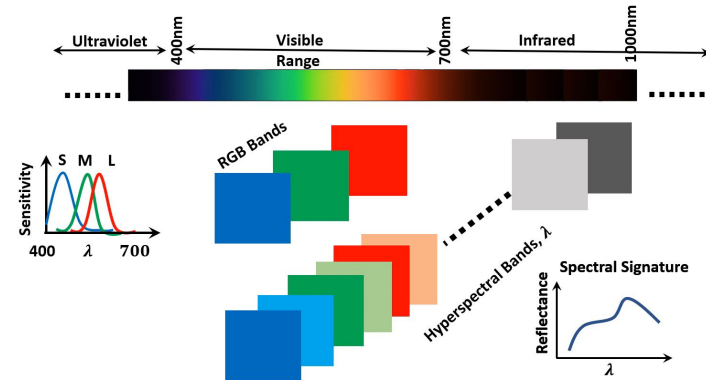


Figure 5     Scientists generally use the remote sensing process when extracting information from remotely sensed data.

### 3.1 Introduction to HSI

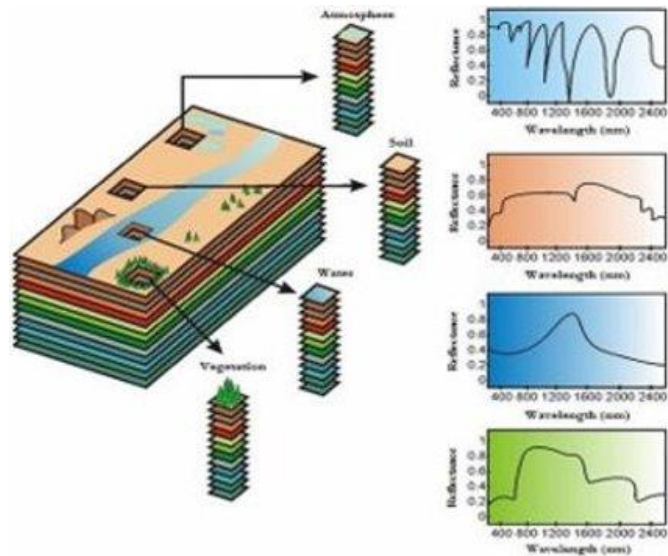
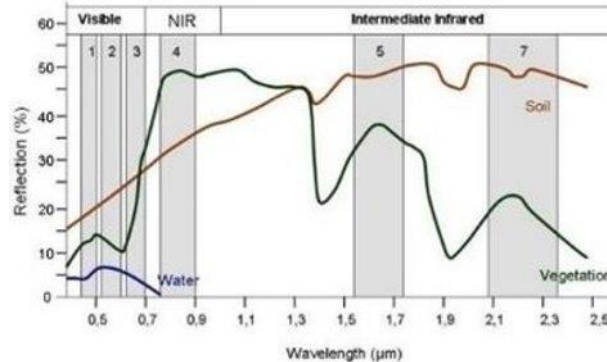
- Hyperspectral (Imaging spectroscopy) - Analysis and evaluation of the reflected (also emitted) radiation detected by a high number of narrow, contiguous and continuous spectral bands.
- Hyperspectral different from that of multispectral instruments thus it produce enormous number of wavebands recorded.
- Geographical area imaged the data produced can be viewed as a cube, having two dimensions that represent spatial position and one that represents wavelength.

### RGB vs Hyperspectral Imaging



## 3.2 Hyperspectral Background

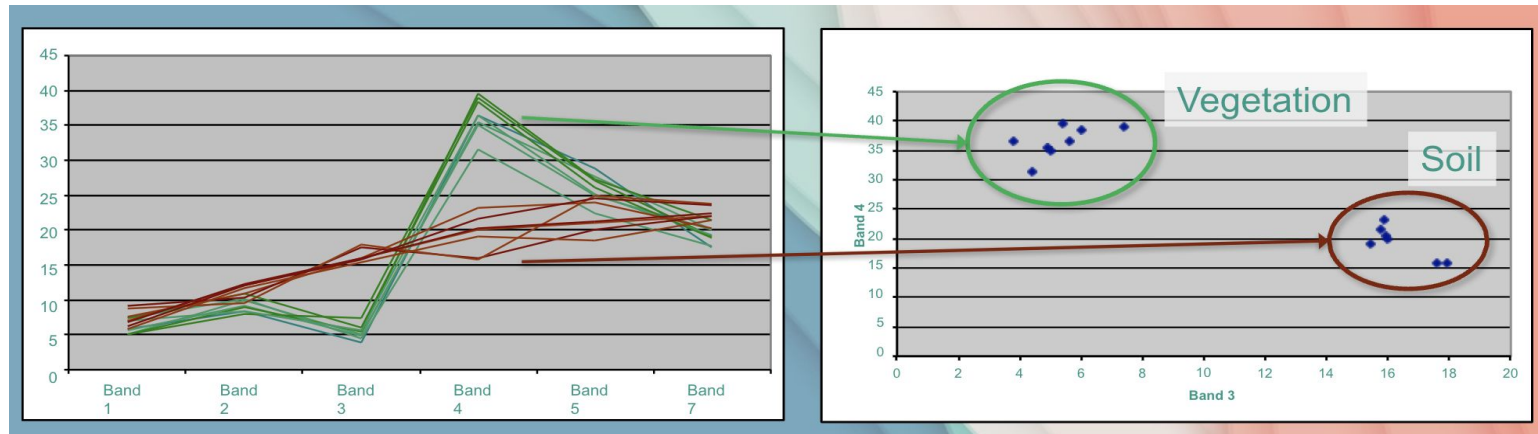
- Capability around for many years, but compute power struggled with large size of data
- That has been overcome and onboard processing is a reality
- Hyperspectral imagery (HSI) usually has at least 30 bands, as compared to multispectral
- Whereas multispectral imagery, like a Landsat image, can give you a class like iron bearing minerals, HSI can give the exact type of mineral



### 3.3 Spectral Signature

- Easier: distinguishing between broad classes
  - e.g. vegetation and soil

- Harder: distinguishing *within* broad classes
  - e.g. vegetation types
- Variation within and between type (broad classes) is below



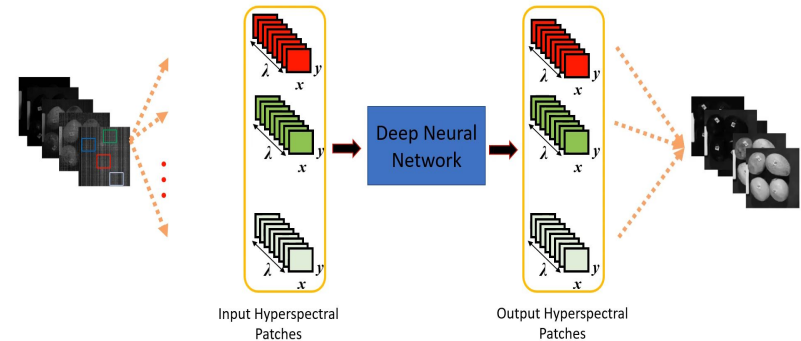
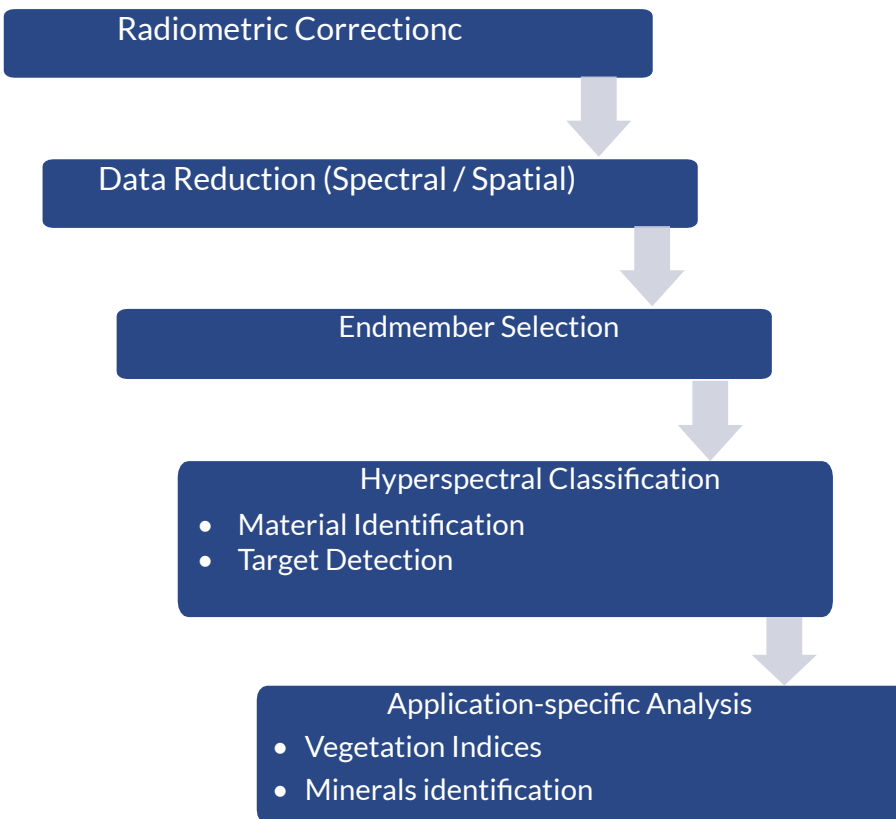
Applied Remote Sensing Training Program

### 3.4 Wavelength Range

Most of the earth surface material have diagnostic absorption feature in the 400-2500 nm range of electromagnetic spectrum. The surface material can be identified if the spectrum is sampled at sufficiently high spectrum.

Bands	Band width	Application
445-670 nm	10-20 nm	Vegetation, water, fe
683-720 nm	5-10 nm	Vegetation/crop/herb
745-765 nm	5-10 nm	Vegetation, atom
780 nm	5-10 nm	veg/atom/pheric correction
880-1035 nm	5-10 nm	Vegetation, fe minerals

## 4. Hyperspectral Image Processing Workflow



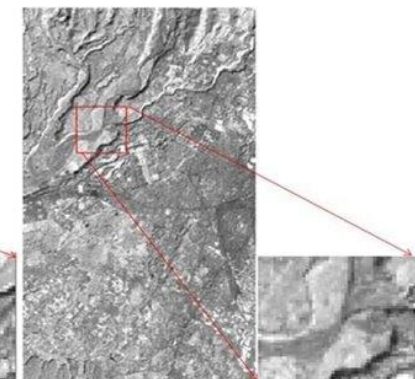
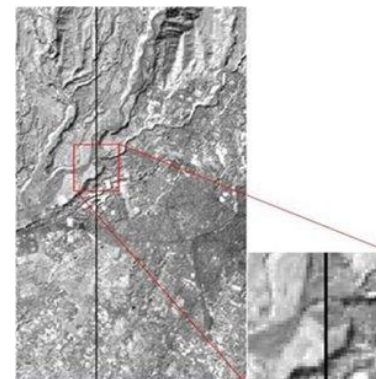
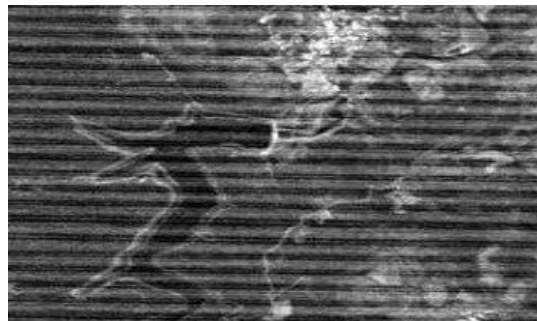
## 4.2 Hyperspectral Data Quality and Issue

Quality of Hyperspectral data is hampered by the noise present in the data. Sources of noise include:-

- i. Sensor calibration
- ii. Sensor drift which results in change of sensor sensitivity over time
- iii. Irradiance variation
- iv. Atmospheric attenuation
- v. Atmospheric path radiance

Types of Noise:

- 1.Bad bands
- 2.Striping errors



# Significance of Very High Resolution Imaging

- Very high-resolution imaging is crucial for critical raw materials, such as lithium and rare earth elements, enabling precise mapping of small deposits and enhancing exploration accuracy in the quest for sustainable and efficient resource extraction.
- Pegmatites are acknowledged as significant sources of lithium, highlighting their geological importance and emphasizing the necessity for targeted exploration to secure a stable supply in the context of the green energy transition.

## 5. Ground-Based HSI

- The historical evolution of ground-based hyperspectral imaging signifies the progressive development of this technology, showcasing advancements that have contributed to its current status as a valuable tool in geological mapping and mineral exploration.



## 5. Ground-Based HSI(2)

SisuROCK is the state-of-the-art workstation for drill core logging. It can acquire data from hundreds of boxes of core per day without any sample preparation. Acquired hyperspectral imaging data can be turned into consistent and objective mineral maps along the core and across the deposit.

### FX10e

FOR 400-1000 nm (VNIR)

- Pyroxene
- Olivine
- Hematite

### SWIR

FOR 970-2500 nm (SWIR)

- OH bearing minerals: clays, phyllosilicates, amphiboles, sulphates
- Carbonates

### FENIX

FOR 380-2500 nm (VNIR + SWIR)

- Same as SWIR
- Hematite, Goethite, Jarosite
- REEs

### FX50

FOR 2.7 - 5.3  $\mu\text{m}$  (MWIR)

- Silicates: quartz, feldspars etc.
- Carbonates and many other minerals seen both in SWIR and LWIR

### RGB

Hi-resolution RGB

- Texture and color

## 5. Ground-Based HSI(3)

- Current challenges and limitations in drone-borne imaging include constraints in weight, operational conditions, and the limited range of short-wave infrared (SWIR) sensors, posing obstacles for achieving comprehensive hyperspectral data coverage in mineral exploration.

## 6. Methodology: Mapping Lithium-Bearing Minerals (4)

The main minerals found in the Uis pegmatites and the range of their characteristic spectral features.

Specifications	Specim AisaFENIX	Specim AisaOWL
Spectral range	380 nm – 2500 nm	7600 nm – 12,300 nm
Spectral sampling (FWHM)	VNIR: 3.4 nm SWIR: 5.7 nm	45 nm
Image size (pixels)	384 pixels per line	385 pixels per line
Spatial resolution	Rock scanner: 1.5 mm Outcrop: ~ 8 cm	Rock scanner: 1.5 mm
Approx. Peak-SNR	VNIR: 600–1000:1 SWIR: 1050:1	450:1
Number of spectral bands	Rock scanner: 450 Outcrop scanning: 620	Rock scanner: 96

Hyperspectral data was collected using the FENIX and OWL sensors, mounted on a tripod in the Uis main pit and on a drill-core scanner/SisuRock setup in the laboratory. Sensors are pushbroom scanners with fixed spectral resolutions (3.5 nm, 12 nm, and 100 nm) and variable spatial sampling (1.5 mm in the rock scanner and ~8 cm in the field setup at a viewing distance of ~60 m).

## 6. Methodology: Study Site

- The study focuses on the V1V2 pegmatite at the Uis tin mine, known for its irregular contacts and unique lithology, making Uis an ideal site for validating hyperspectral imaging in mineral exploration.
- The V1V2 pegmatite deposit at the Uis tin mine in Namibia has recently declared lithium oxide reserves, surpassing 450 Kt.

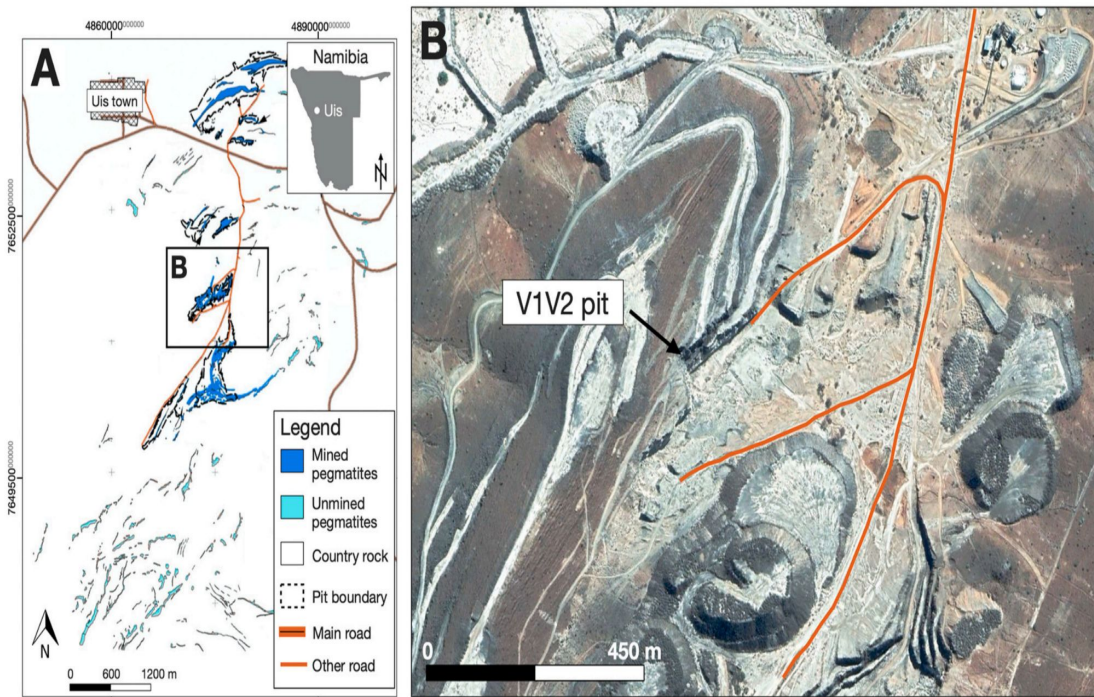
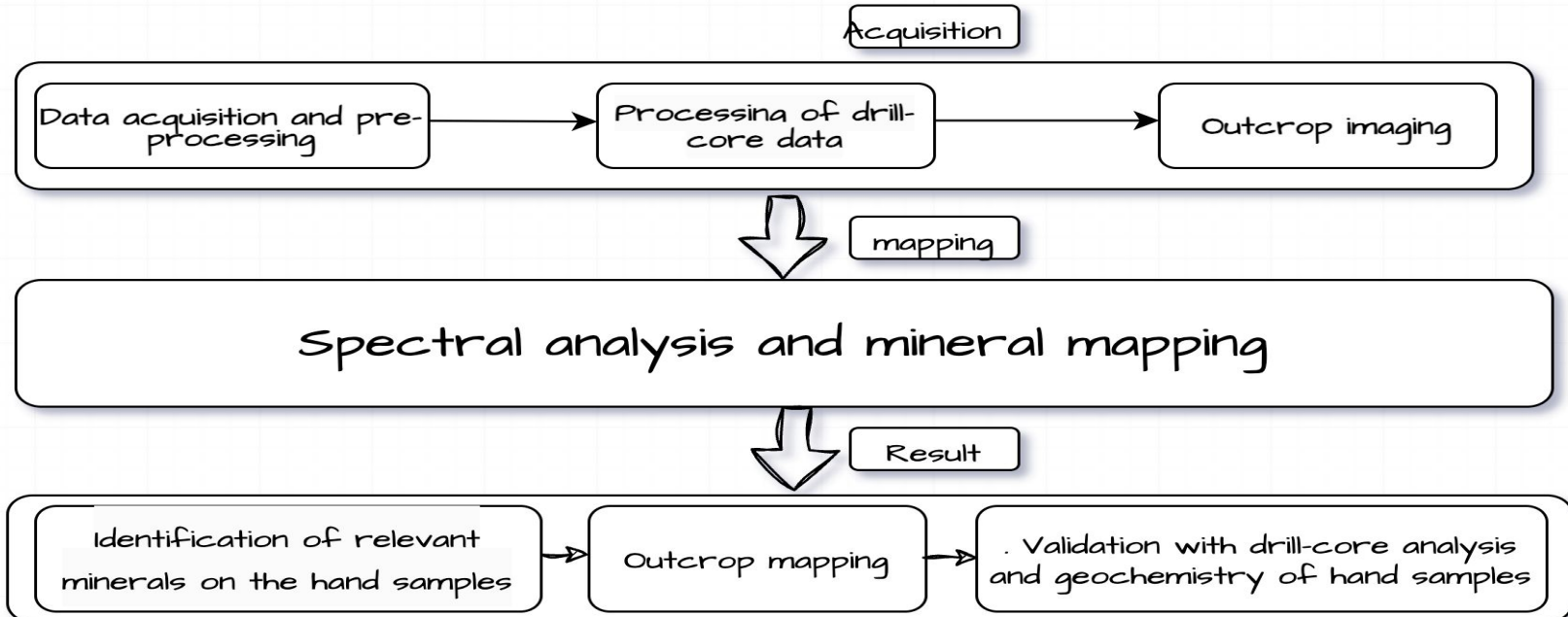


Fig. 1. Study site. (A) Geological map of the Uis Tin mine showing the mapped pegmatites and the location of the main pit. (B) A satellite image of the main V1V2 pit (Google, CNES, Airbus, 2021).

## 6. Methodology: Rough Sketch(2)



Acquired hyperspectral data by scanning 16 meters of drill-core and 8 hand samples from the main pit at Uis using both the FENIX and OWL sensors in a SiSuRock scanner configuration. The laboratory setup provided optimized conditions for high signal-to-noise ratio and spatial sampling.

## 6. Methodology: Data processing(2)

### Preprocessing:

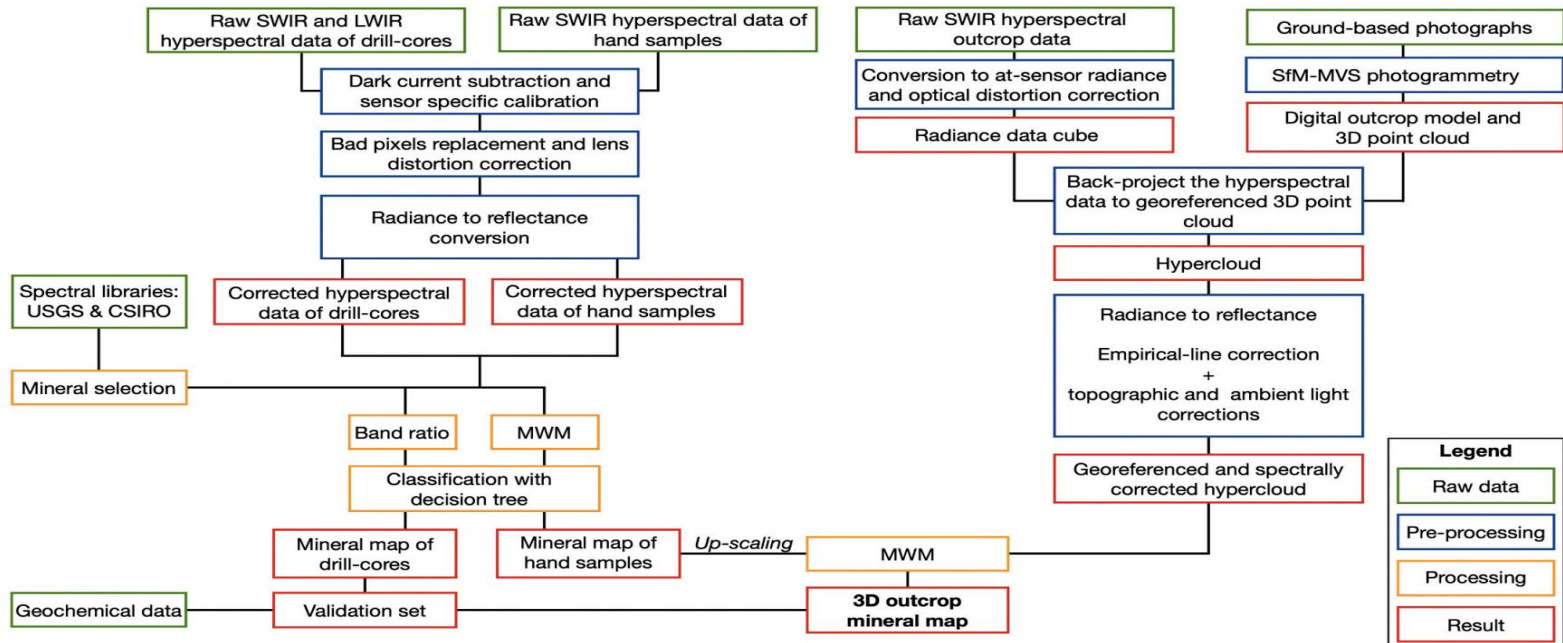
- Calibration using We used in-house Python toolboxes, Hylite and Mephysto.
- Bad Pixel Replacement Replaced by the median of the surrounding pixels
- Lens Distortion Correction was corrected to create planimetric images of the scanned samples
- Reflectance Estimation: Radiance measurements were converted to reflectance estimates by dividing the data with measurements from white Spectralon R90 calibration panel (for FENIX) and brushed aluminum panel (for OWL).

### Outcrop Imaging:

Due to administrative constraints on LWIR sensors, only the FENIX was used for outcrop scans in Namibia.

- Georeferencing
- Hyperspectral-Photogrammetry Fusion
- Topographic Corrections

## 6. Methodology: Flow(3)



The workflow involves processing raw hyperspectral VNIR-SWIR and LWIR datasets from laboratory drill-cores and hand samples, combined with field-acquired hyperspectral scans and photographs, for mineral mapping and geological interpretation.

## 6. Methodology: Mapping Lithium-Bearing Minerals (5)

Table 3

The main minerals found in the Uis pegmatites and the range of their characteristic spectral features.

Minerals in the Uis pegmatites	Characteristic spectral range
Feldspar (predominantly albite and microcline with minor amounts of plagioclase and orthoclase)	LWIR
Quartz	LWIR
Muscovite (and minor amounts of other micas)	SWIR and LWIR
Cookeite	SWIR
Clay minerals (trace amounts)	SWIR and LWIR
Montebrasite (trace amounts)	SWIR

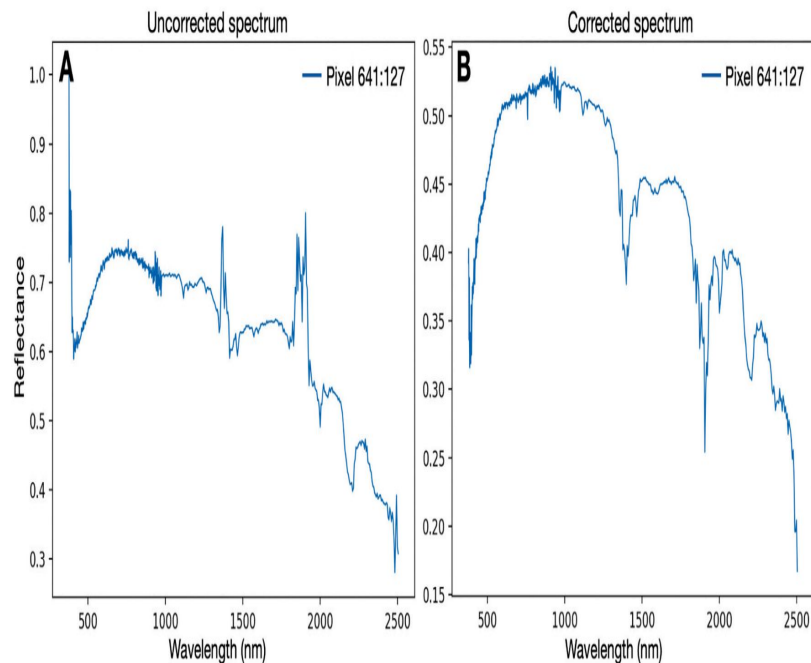


Fig. 5. Example of a spectrum captured during field acquisition with the AisaFENIX showing before and after corrections. (A) Uncorrected spectrum (only ELC applied). (B) After a joint topographic and atmospheric correction.

## 6. Methodology: VNIR-SWIR spectra of samples

- (A) Iron-bearing alteration mineral spectrum.
- (B) Ammonium clay/mica spectrum.
- (C) Amblygonite group mineral spectrum.
- (D) Possible buddingtonite spectrum.
- (E) Muscovite/white mica spectrum.
- (F) Cookeite spectrum.

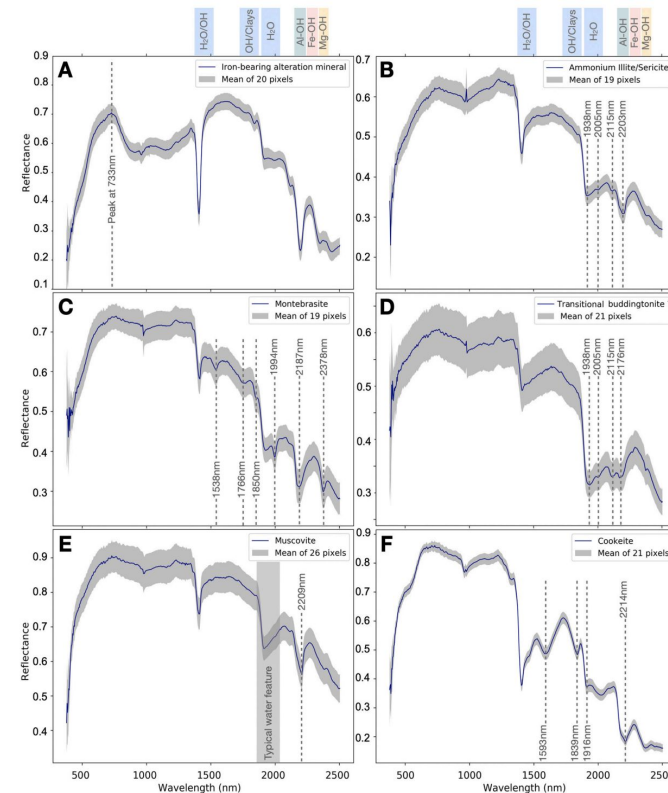


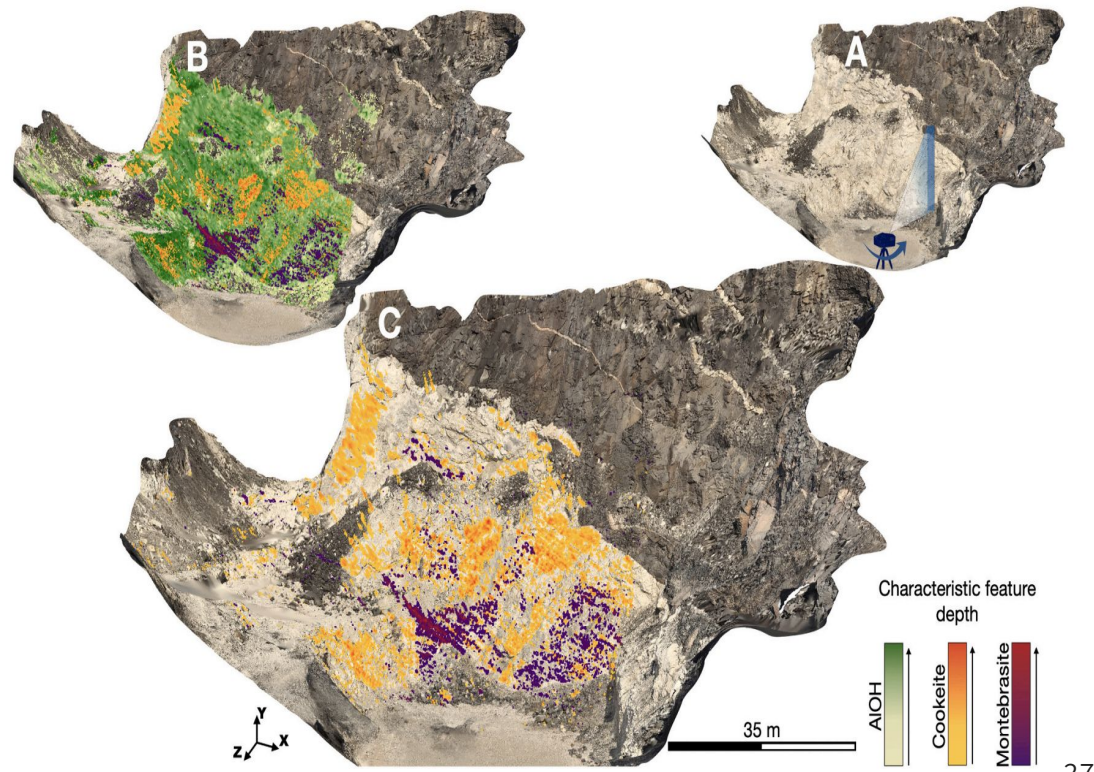
Fig. 6. VNIR-SWIR spectra of minerals from the hand samples captured by the AisaFENIX. (A) Iron-bearing alteration mineral spectrum. (B) Ammonium clay/mica spectrum. (C) Amblygonite group mineral spectrum. (D) Possible buddingtonite spectrum. (E) Muscovite/white mica spectrum. (F) Cookeite spectrum.

## 6. Methodology: Mapping Lithium-Bearing Minerals

(A) RGB 3D model of the V1V2 pit indicating the location of the FENIX sensor.

(B) Hypercloud minimum wavelength map showing the mineral abundances overlain onto the 3D model

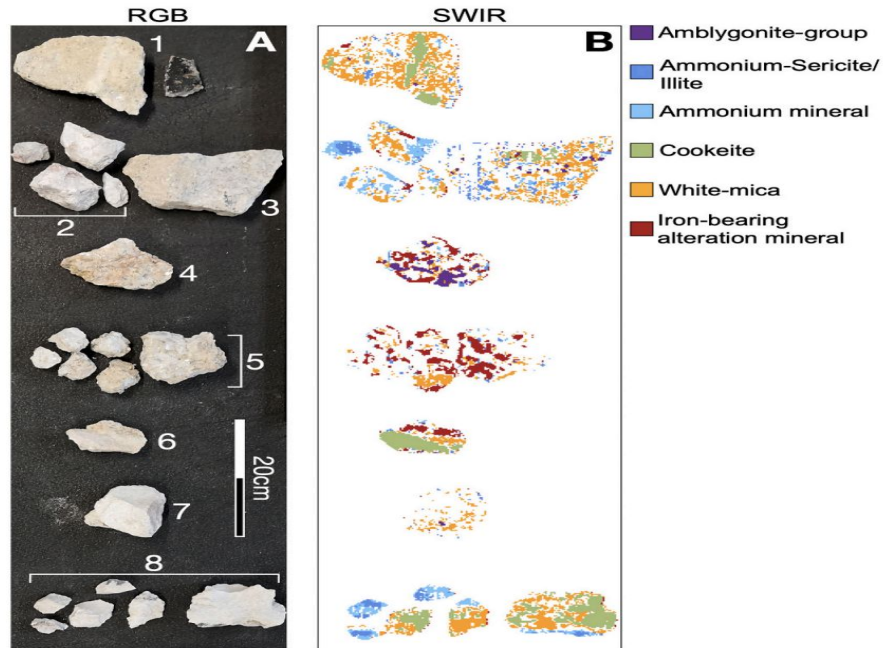
(C) only the Li-bearing minerals. The colour corresponds to the composition or characteristic mineral absorption feature mapped and the intensity indicates the depth of the feature.



## 6. Methodology: Decision tree results

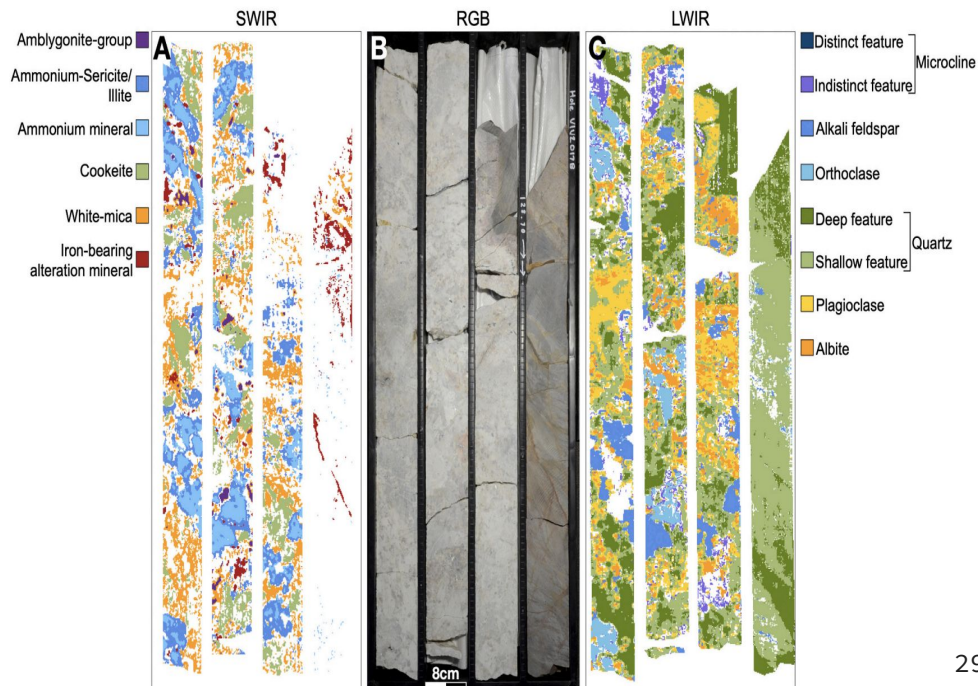
(A) RGB photograph indicating the sample number that corresponds to the XRD results.

(B) Mineral map of the VNIR SWIR active minerals.



## 6. Methodology: Verification

- (A) Mineral map: VNIR-SWIR active minerals captured by the AisaFENIX.  
(B) RGB photograph of box 1.  
(C) Mineral map of the LWIR active minerals captured by the AisaOWL.

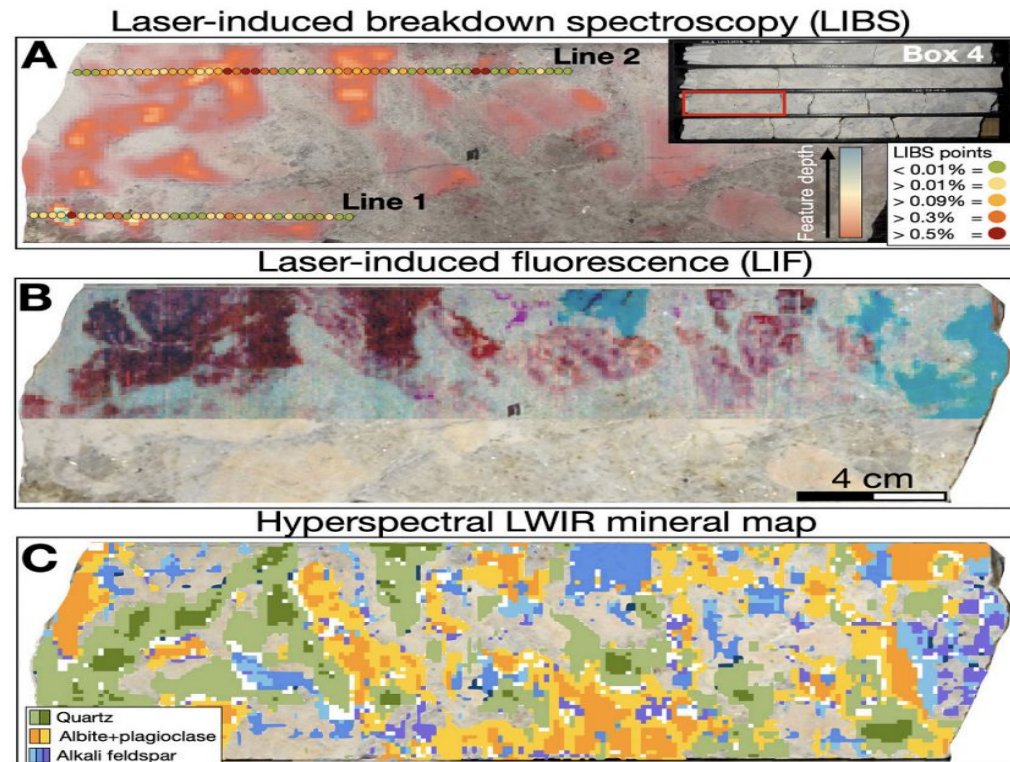


## 6. Methodology: (Verification)

(A) Mineral map of the VNIR-SWIR active minerals captured by the AisaFENIX.

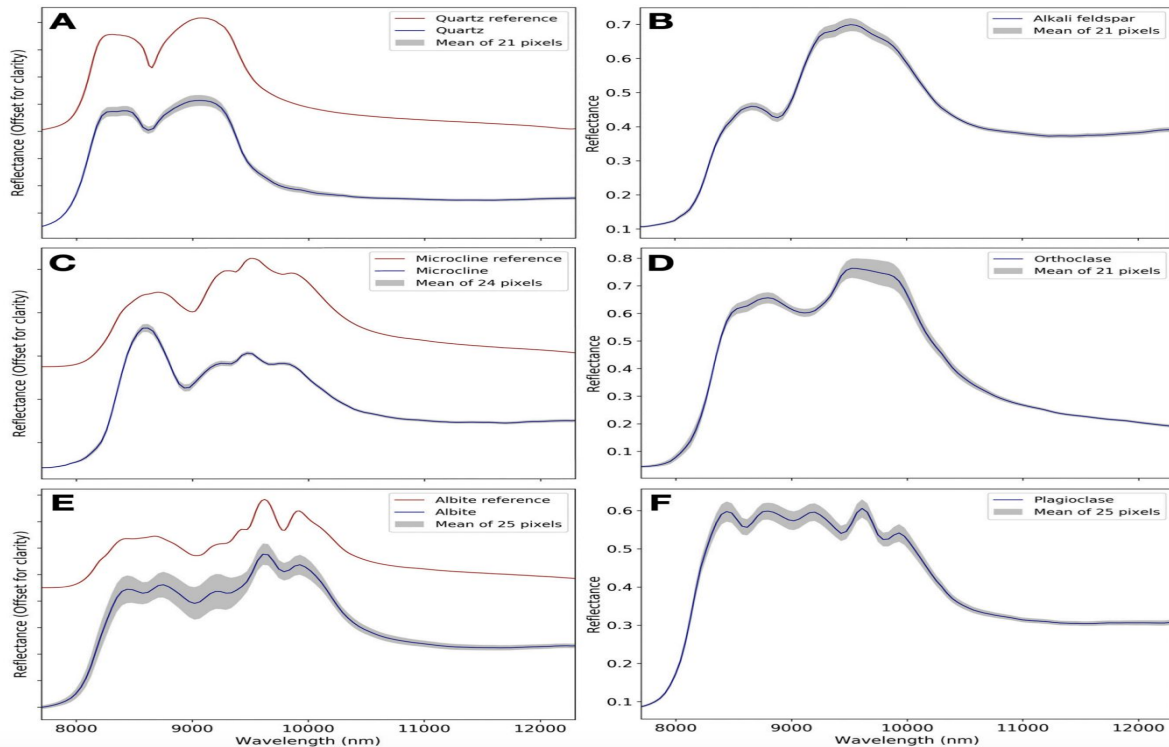
(B) RGB photograph of box 4.

(C) Mineral map of the LWIR active minerals captured by the AisaOWL.



## 7. Results -comparison

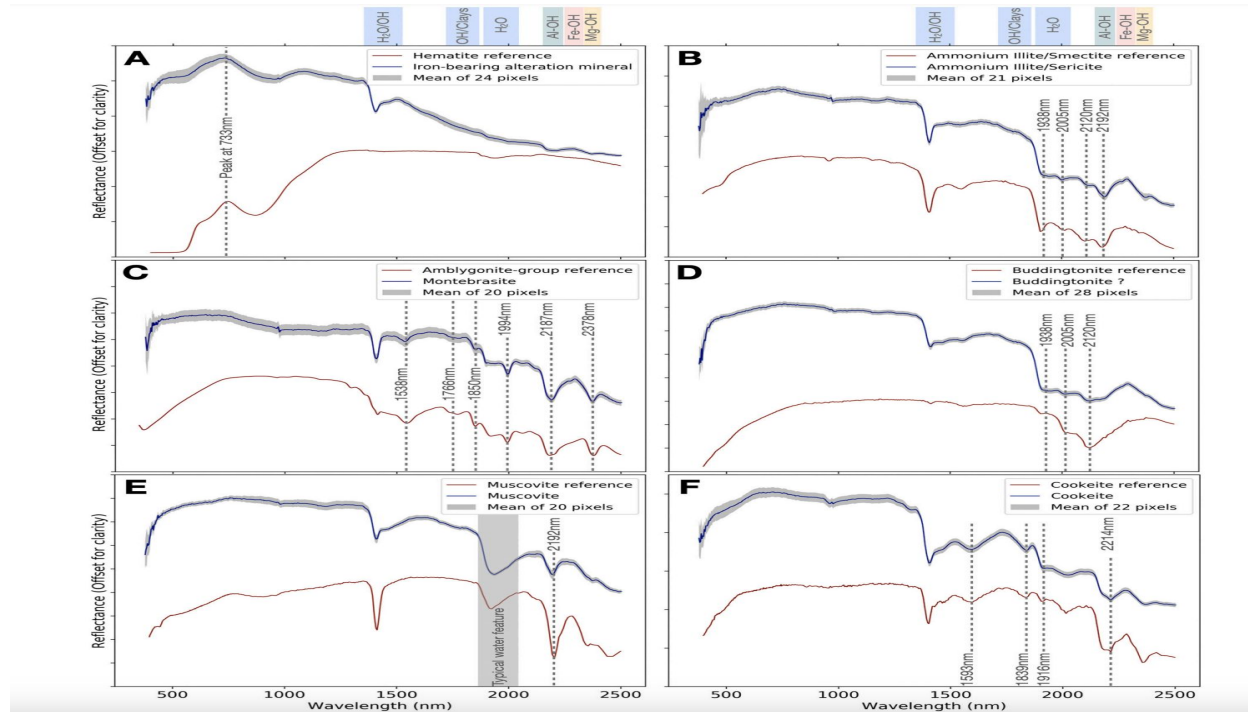
Drill-cores captured by the AisaFENIX compared with reference spectra taken from the CSIRO spectral library



- Validation of accuracy using drill-core data, XRD analysis, and LIBS measurements

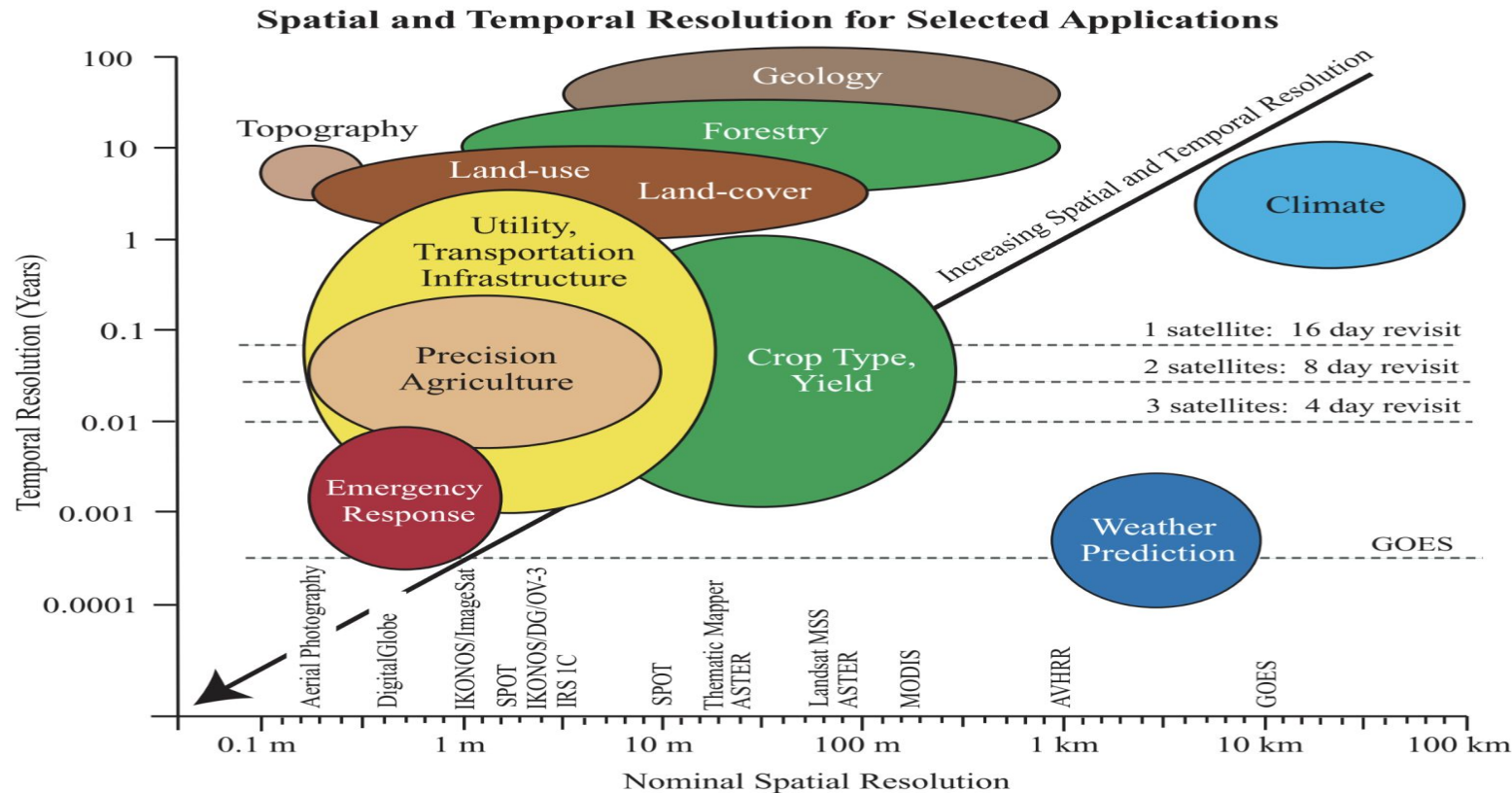
## 7. Results - Comparison

Drill-cores captured by the AisaOWL compared with reference spectra taken from the USGS spectral library



- Application of the method for efficient mapping of complex terrains

## 8. Future Directions



## 9. Limitation of the paper

- LWIR Sensors
- UAV
- Limited Mineral Libraries

## 9. Advantages of the paper

- Mineral Identification
- Library Comparison
- Mapping Techniques

# Machine Learning Method

- Feature Extraction
- Enhanced Classification
- Algo for Ultraspectral imaging
- Cheaper way for acquisition of hyperspectral image.

## References:

- AfriTin Mining Ltd., 2019. Maiden JORC resource at Uis. In: Alternative Metal Market. London Stock ExchangeRNS number: 3635M.
- Ali, S.H., Giurco, D., Arndt, N., Nickless, E., Brown, G., Demetriades, A., Durrheim, R., Enriquez, M.A., Kinnaird, J., Littleboy, A., Meinert, L.D., 2017. Mineral supply for sustainable development requires resource governance. *Nature* 543 (7645), 367–372.
- Ashworth, L., Kinnaird, J.A., Nex, P.A.M., Erasmus, R.M., Przybylowicz, W.J., 2018. Characterization of fluid inclusions from mineralized pegmatites of the Damara belt, Namibia: insight into late-stage fluid evolution and implications for mineralization. *Mineral. Petrol.* 112, 753–765.
- Beran, A., 2002. Infrared spectroscopy of micas. *Rev. Mineral. Geochem.* 46 (1), 351–369.
- Boesche, N.K., Rogass, C., Lubitz, C., Brell, M., Herrmann, S., Mielke, C., Tonn, S., Appelt, O., Altenberger, U., Kaufmann, H., 2015. Hyperspectral REE (rare earth element) mapping of outcrops—applications for neodymium detection. *Remote Sens.* 7 (5), 5160–5186.
- Boysen, R., Jackisch, R., Lorenz, S., Zimmermann, R., Kirsch, M., Nex, P.A.M., Gloaguen, R., 2020. Detection of REEs with lightweight UAV-based hyperspectral imaging. *Sci. Rep.* 10 (1), 1–12.



# Thank you